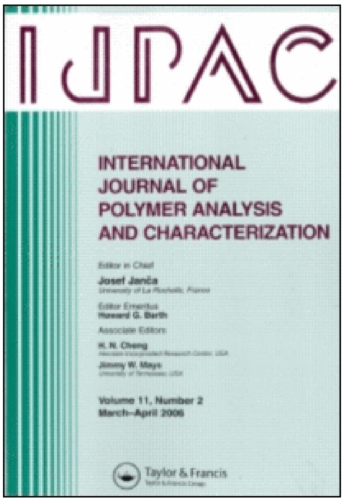

International Journal of Polymer Analysis and Characterization
Publication details, including instructions for authors and subscription information:
http://www.informaworld.com/smpp/title~content=t713646643

# Characterization and Studies of Designed Photodefinable CoPoly(amic Acid) Ionic Salt Solutions

Rohitkumar H. Vora[a]; P. Santhana Gopala Krishnan[a]; S. Veeramani[a]
[a] Polyimide Project Group, Advanced Polymers and Chemicals Cluster, Molecular and Bio-Materials Laboratory, Institute of Materials Research and Engineering (IMRE), Singapore

**To cite this Article** Vora, Rohitkumar H. , Krishnan, P. Santhana Gopala and Veeramani, S.(2004) 'Characterization and Studies of Designed Photodefinable CoPoly(amic Acid) Ionic Salt Solutions', International Journal of Polymer Analysis and Characterization, 9: 1, 177 — 196
**To link to this Article: DOI:** 10.1080/10236660490891320
**URL:** http://dx.doi.org/10.1080/10236660490891320

*International Journal of Polymer Anal. Charact.*, 9: 177–196, 2004

ISSN: 1023-666X print
DOI: 10.1080/10236660490891320

# *Characterization and Studies of Designed Photodefinable CoPoly(amic Acid) Ionic Salt Solutions*

**Rohitkumar H. Vora,**
**P. Santhana Gopala Krishnan, and**
**S. Veeramani**
Polyimide Project Group,
Advanced Polymers and Chemicals Cluster,
Molecular and Bio-Materials Laboratory,
Institute of Materials Research and Engineering
(IMRE), Singapore

*In an attempt to develop a very stable photodefinable ionic salt solution, we synthesized two series of co-poly(amic acid)s (CoPAAs) by reacting 3,3′,4,4′-biphenyl tetracarboxylic dianhydride (BPDA) or 3,3′,4,4′-benzophenone tetracarboxylic dianhydride (BTDA) with various mole percents of ortho-Tolidine (o-TDA) and 1,3-bis(3-aminopropyl) tetramethyl disiloxane (SiDA). Subsequently, two series each of the ionic bond type photodefinable co-poly(amic acid) salts (CoPAS) were made, using 2-(diethylamino)ethyl methacrylate (DEEM) and 2-(dimethylamino)ethyl methacrylate (DMEM). NMR studies were carried out on bisphthalamic acid of o-TDA and SiDA model compounds to identify weak linkage in the above PAAs. Bulk viscosity, inherent viscosity, acid number, and molecular weight of CoPAA and CoPAS solutions decreased drastically as the storage time increased. CoPAS was less stable than CoPAA. BPDA-based PAA showed less viscosity drift than*

Received 7 June 2004; accepted 13 July 2004.

The authors would like to thank Dr. S. Vivekanandan, Department of Biological Sciences, National University of Singapore for the useful suggestions with regard to NMR analysis. The authors also acknowledge with sincere gratitude and thanks for the materials (*o*-TDA diamine) support provided by the Wakayama Seika Kogyo Co. Ltd., Japan.

Address correspondence to Rohitkumar H. Vora, Advanced Polymers Research and Technologies, 505 Cinder Rd., Edison, NJ 08820, USA. E-mail: rohitvora@apr-technologies.com

*the BTDA-based PAA. Both CoPAA and CoPAS samples showed a two-step weight loss in air atmosphere. The first step was attributed to imidization and the second step to thermal degradation. The activation energy for thermal degradation was determined using Coats-Redfern and Chang methods and the values were found to be comparable.*

*Keywords*: Photodefinable polyimides; Poly(amic acid); Poly(amic acid) ionic salt; Amic acid ionic salt; Viscosity stability and Thermal degradation studies

## INTRODUCTION

Polyimides (PI)s have inherently high mechanical properties, good chemical resistance, low dielectric constant, and high thermal stability. Hence, they are used in microelectronics, automotive, and aerospace applications[1]. In microelectronics, the high-resolution photolithography technique is used for the fabrication of complex miniaturized electronics circuit and components such as VLSI and multichip devices[2–3]. In photolithography applications, the formulations containing photodefinable poly(amic acid) (PDPAA) derived from PI precursors and photosensitizers greatly simplify the complex microelectronic fabrication process[4]. In the development of photosensitive or photodefinable polyimides (PDPI), it is clearly understood that structural rigidity of dianhydrides contributed to the increase in the glass transition temperatures and some of the conventional PIs are insoluble; there are no suitable processing methods available to process such as high $T_g$ and insoluble materials. Due to these limitations, research was focused on the modification of the backbone structures of PIs. There are several approaches available in literature, such as incorporation of a flexible ether or isopropylidene linkage between dianhydrides and diamine structure and *meta* oriented phenoxyphenyl rings in the diamine[3–9]. Another approach is through incorporation of certain low percentage of siloxane moieties without affecting other desired properties. Such incorporation of siloxane moieties in polymer backbone would impart a number of additional benefits to the polymeric system, such as reduced water absorption, high gas permeability, low dielectric constant, good resistance to oxygen environment at high temperature, modified surface adhesion properties, and flame resistance.

Commercially, PDPAA is available in ester (positive acting) or ionic salt (negative acting) form[4]. The ionic salt, known as poly(amic acid) ionic salt (PAS), is derived by reacting PAA solution with tertiary amines containing acryloyl or methacryloyl groups, such as 3-(dimethylamino)propyl methacrylate (DMPM), 2-(dimethylamino)ethyl methacrylate (DMEM) and 2-(diethylamino)ethyl methacrylate (DEEM)[4,8–13]. PI precursors are almost the main ingredient in the negative-acting PDPAA formulation and are relatively unstable upon prolonged storage, even at refrigeration conditions. They are known to undergo various reactions[2,5]. These reactions not only affect the inherent properties of PAA and PAS but those of the resulting PIs as well. To prevent or to minimize the degradation of PAA and PAS, it is important to know the reaction that is taking place during storage. Hydrolysis of PAA derived from [3,3,4,4′-biphenyl tetracarboxylic dianhydride (BPDA) + *p*-phenylene diamine (PPD)][6] and [pyromellitic dianhydride (PMDA) + 4,4′-oxydianiline (ODA)][6–8], and the effect of moisture on stability of certain [4,4′- oxydiphthalic anhydride (ODPA) + *m*-tolidine (*m*-TDA)] and [ODPA + *o*-tolidine (*o*-TDA)] PAA have been reported[11–13]. However, there is no information available on the storage or thermal stability of their photodefinable ionic salt solutions containing methacrylate groups, even though the structure-property relationship[14–16] and their lithographic performance[17,18] have been well documented. In this work, we have specifically designed two amic acid model compounds and two series of co-poly(amic acid)s (CoPAA) and their salt solutions (CoPAS). The storage stability studies were carried out on model compounds both with and without the presence of added water at room temperature (RT) using $^1$H-NMR (nuclear magnetic resonance). The storage stability of PAA, CoPAA, and CoPAS were studied as a function of storage time. Thermal behavior of CoPAA and CoPAS solids and resulting CoPI films was also investigated, and the results are discussed here.

# EXPERIMENTAL

## Materials

Electronic-grade powdered BPDA and 3, 3′, 4, 4′-benzophenone tetracarboxylic dianhydride (BTDA) were obtained from Chriskev Co. (USA); PA was purchased from BDH Laboratory (UK); *o*-TDA was received from Wakayama Seika Kogyo Co. (Japan); 1,3-bis(3-aminopropyl) tetramethyl disiloxane (SiDA) was obtained from Tokyo Kasei Organic Chemicals Co. (Japan); N-methyl-2-pyrrolidone (NMP) was purchased from Lab-Scan (Singapore); phosphorous pentoxide ($P_2O_5$), dichloromethane (DCM), acetone, tetrahydrofuran (THF), dimethyl acetamide (DMAc), N,N-dimethyl formamide (DMF), dimethyl sulfoxide (DMSO), $\gamma$-butyrolactone (BLO), and tetramethyl ammonium hydroxide ($\sim$25% in methanol) (TMAH) were obtained from Aldrich Chemical Company (USA). All the solvents except NMP were used as received. NMP was freshly distilled over $P_2O_5$, under reduced

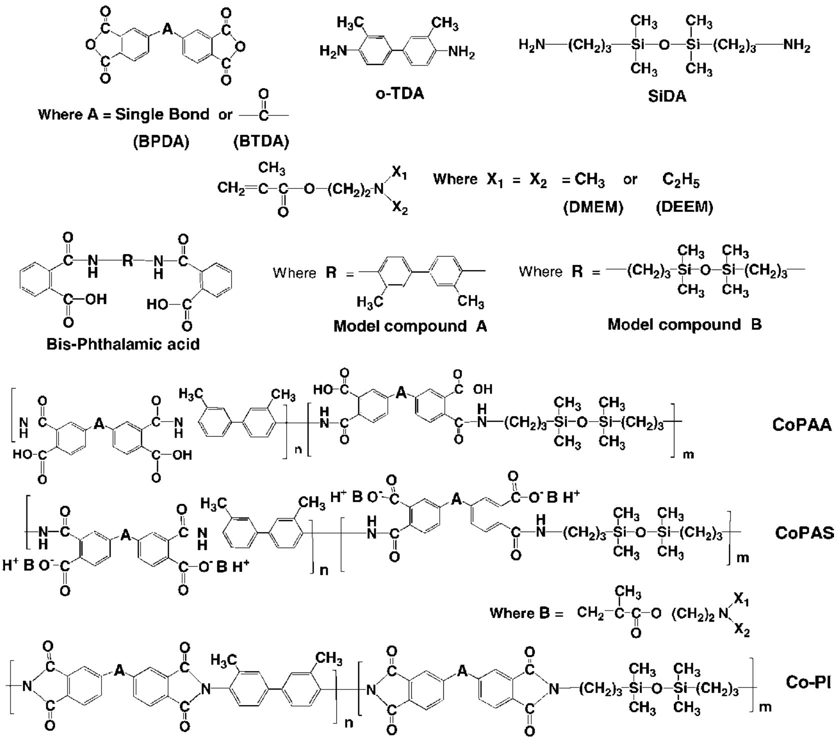

FIGURE 1 Chemical structure of monomers, model compounds A and B, and repeat unit of co-poly(amic acid) (CoPAA), ionic salt of poly(amic acid) (CoPAS), and co- polyimide (CoPI).

pressure and stored over pre-dried molecular sieves and used when needed. Both dianhydrides were dried in an oven at 150 ± 2°C, and o-TDA was dried at 55 ± 2°C overnight. Other chemicals were used as received. The chemical structures of monomers used are shown in Figure 1.

## Synthesis of Polyamic Acid (PAA), Copoly(amic Acid) (CoPAA), and Photodefinable Ionic Salt Formulation (CoPAS)

From several methods for the preparation of PIs reported in the literature[19–23], a two-step method[23] was used the in this investigation.

### *PAA and CoPAA*

A typical procedure for the synthesis of PAA from BPDA and *o*-TDA is given as follows. In a 500 mL three-neck round-bottom glass reactor unit fitted with a mechanical stirrer and inert environment, 29.42 g (0.10 mol) of solid BPDA powder was added in installments to an equimolar amount of *o*-TDA (21.23 g), which is pre-dissolved in NMP to make 20 wt% solution. The reaction mixture was stirred at RT overnight to make viscous solutions, filtered and packed in a polypropylene bottle under an argon environment, and stored in a refrigerator prior to the preparation of their ionic salt solutions. A small amount of the solution was withdrawn and precipitated in deionized water for differential scanning calorimetry (DSC), X-ray diffraction (XRD) and thermogravimetric analysis (TGA). A similar procedure was followed for the preparation of all CoPAAs. The chemical structures of repeat unit of PAAs and CoPAAs are given in Figure 1.

### *PAS and CoPAS Solution*

Two series of photodefinable ionic salt CoPAS were synthesized from the precursors, i.e., PAA and CoPAA of the BTDA and BPDA. The chemical structures of their repeat units are given in Figure 1. To PAA/CoPAA solution, a stoichiometric amount of DEEM or DMEM was added based on the calculation of theoretical mol percent of free carboxylic acid groups on the polymer chain from the chemical structure repeat unit. The solution was stirred in nitrogen environment at RT for two hours and then packaged in a polypropylene bottle under argon environment for further study.

Since ionic salts are generally soluble in water, both PAS and CoPAS solids were precipitated by reverse precipitation in acetone instead of in deionized water at RT and were chopped to small particles in a high-speed blender. They were washed several times with fresh acetone and vacuum dried overnight at RT.

## Model Compounds Synthesis

To identify the weak linkage in PAA and CoPAA, two bisphthalamic acid model compounds, A and B, were synthesized whose chemical structures were derived from the chemical structure of CoPAA. The chemical structures of model compound A and B are given in Figure 1.

### *Synthesis of model compound A (Bisphthalamic Acid of 3,3′-dimethyl 4, 4′-diaminobiphenyl)*

In a 500 mL round-bottomed flask fitted with a magnetic stirrer, *o*-TDA (10 g, 47.2 mmol) was dissolved in 400 mL DCM. PA (13.97 g, 94.3 mmol) was gradually added to the solution and the mixture was stirred overnight at RT. Bisphthalamic acid appeared as a dense white precipitate. It was filtered and dried at RT overnight in nitrogen atmosphere, and 22.12 g of dry model compound A was obtained with a yield of 92.3%.

### *Synthesis of model compound B (Bisphthalamic acid of 1,3-bis (3-propyl) tetramethyl disiloxane)*

Two grams of SiDA in 23 mL of THF was dissolved using a magnetic stirrer in a 50 mL single-necked round-bottomed flask fitted with a calcium chloride guard tube. Then 2.6 g of freshly dried PA was gradually added into the above diamine solution in small increments, and the solution was stirred overnight at RT. The next morning, the model compound was precipitated out from hexane and the mixture was kept in a refrigerator. White crystalline solid of compound B appeared at the bottom of flask and it was filtered. The trapped solvent in the crystals was removed by applying vacuum at 40°C in an oven for a few hours and 3.6 g of the product was obtained with a yield of 81.7%.

## PI and Co-PI Film Preparation

In this study, the PAA and CoPAA solutions were coated on glass plates using a Gardner film casting knife (Model AG-4300, Pacific Scientific, USA) with adjustable gate clearance controlled with a micrometer from 0 to 12.5 mm gap. The films were dried in a nitrogen environment for an hour and then heated gradually in a programmable oven. The curing cycle used was 80°C (1 h), 100°C (1 h), 150°C (1 h), 200°C (1 h), 225°C (1 h), 250°C (1 h), and 300°C (1 h). Yellow to amber color films of PI and Co-PI films were obtained. Films were found to be self-supporting or brittle with average thickness of 25 to 27.5 μm.

# CHARACTERIZATION

$^1$H-NMR spectra were recorded using a Bruker 400 MHz NMR spectrometer at RT using DMSO-d6 as a solvent. $^1$H NMR studies were conducted immediately, after 8 h and one week on model compounds containing 0, 10, and 20% of water by weight at RT.

Mass spectrum was recorded using a Micromass VG 7035 for electron impact (EI) ionization mode. The ionization potential used for EI mode was 70 eV.

Inherent viscosity at a concentration of 0.5 g/dL of PAA, CoPAA, and CoPAS was determined according to ASTM 2515/D446 using a Schott-Gerate model AVS360 and capillary viscometer type DIN Ubbelohde at 25°C in NMP. An average of three readings was taken for the calculation. Bulk viscosity of PAA, CoPAA, and CoPAS was determined using a programmable rheometer, Brookfield model DV-III (with Rheocalc software and Brookfield water bath model TC-200/500) at 5 rpm using CP42 spindle. An average of six readings was reported.

Relative molecular weights $[\overline{M}_n, \overline{M}_w]$ of PAA, CoPAA, and CoPAS with respect to polystyrene standards were measured by gel permeation chromatography (GPC), as per the procedure reported in literature[24]. A GPC system having Waters 2690 separation module and Waters 2487 UV detector was used. Three Gelpack GL-S300MDT-5 (Hitachi) columns of size 8 × 300 mm, packed with polystyrene gel having an exclusion limit of $2 \times 10^8$, were connected in series and housed in an oven maintained at 40°C. A mixture of THF: DMF (1:1) containing 0.06 M LiBr and 0.06 M $H_3PO_4$ was used as mobile phase to suppress a polyelectrolyte effect typically observed for poly(amic acid)/polyimides type of polymers. The mobile phase was filtered through a 0.2 μm PTFE filter (Millipore). Conditions used were wavelength 270 nm, flow rate 1 mL/min, injection volume 200 μL and sample concentration 1 mg/mL. The polymer samples were pre-dissolved in above eluent mixture and filtered through a 0.45 μm PTFE-PP 13 mm filter (Lida Manufacturing) just prior to injection. Ten polystyrene standards (Polysciences Corporation, USA) having molecular weights ranging from 4 to 2000 K were used for calibration.

The acid number of PAA, CoPAA, and CoPAS solutions was determined by titrating with tetramethyl ammonium hydroxide (TMAH) using a TitroLine alpha (model TZ 2055) (Schott-Gerate GmbH) automatic potentiometric titrator fitted with a magnetic stirrer base (model TM125) and is reported as mg of TMAH per gram of solution. The electrode used was filled with LiCl/glacial acetic acid solution (model SAN 6480). It must be noted that the acid number determined for Co-PAS is not only for the free acid present but also for the carboxylic acid attached to the tertiary amine, i.e., DEEM or DMEM. This is the limitation of this method.

Wide-angle X-ray diffraction measurements (WAXD) of PAA, CoPAA, PAS, and CoPAS were carried out using solid samples on an X-ray diffractor unit (Phillips model PW 1729-10) fitted with Cu - K$\alpha$ radiation (30 kV, 20 mA) with wavelength $\lambda$ of 1.54 Å. The scanning rate was 0.5°/min at RT. The spectral window ranged from $2\theta = 10°$ to $30°$.

Solubility of PI and Co-PI films was determined by dipping $1 \times 1\,\text{cm}^2$ film samples in capped vials containing selected solvents and kept on at RT. The extent of solubility was evaluated after 24 h.

The glass transition temperatures ($T_g$) of PI and Co-PI films were determined using differential scanning calorimeter (DSC) model DSC-2920 (TA Instruments). Scans were run from RT to 450°C at a heating rate of 20°C/min in flowing nitrogen atmosphere (10 cc/min).

Thermal decomposition temperatures (5% weight loss) of samples of PAA, CoPAS solids, and PI and CoPI films were determined using a dynamic thermogravimetric analyzer (TGA) (Perkin Elmer model TGA-7 with Pyris software). Scans were run from 50 to 800°C at a heating rate of 10°C/min in a flowing air atmosphere (10 mL/min).

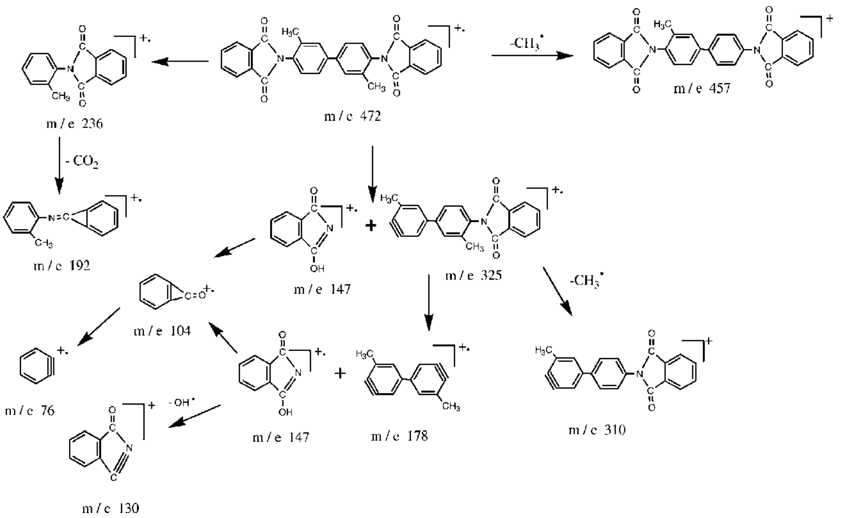

**FIGURE 2** EI mass fragmentation pattern for model compound A.

# RESULTS AND DISCUSSION

## Mass Spectrometric Analysis of Model Compound A and B

In EI mode, the molecular ion peak of bisphthalamic acid model compounds A and B was not observed at 508 and 544 respectively. But a peak was observed at 472 and 508 for amic acids A and B respectively, corresponding to their imide. Obviously, the amic acid had imidized during ionization by electron impact. A similar observation was made for other amic acid compounds[11,13]. Mass fragmentations of compound A and B are given in Figures 2 and 3 respectively.

## Stability Study of Model Compounds by NMR Spectroscopic Analysis

Chemical structures of the compounds A and B given in Figure 1 were confirmed from the $^1$H NMR spectra and the chemical shift values are given in $\delta$ (ppm):

- Compound A: $^1$H-NMR (DMSO-$d_6$) $\delta$ 2.02 (Ar-$CH_3$), $\delta$ 7.0– 8.0 ($Ar$), $\delta$ 10.36 (N$H$), and $\delta$ 12.9 (COO$H$).
- Compound B: $^1$H-NMR (DMSO-$d_6$) $\delta$ 0.1 ($CH_3$), $\delta$ 0.55 ($CH_2$-NH), $\delta$ 1.0 (Si-$CH_2$), $\delta$ 1.5 ($CH_2$-$CH_2$-$CH_2$), $\delta$ 7.2– 7.8 ($Ar$), $\delta$ 8.3 ($NH$), and $\delta$ 12.9 (COO$H$).

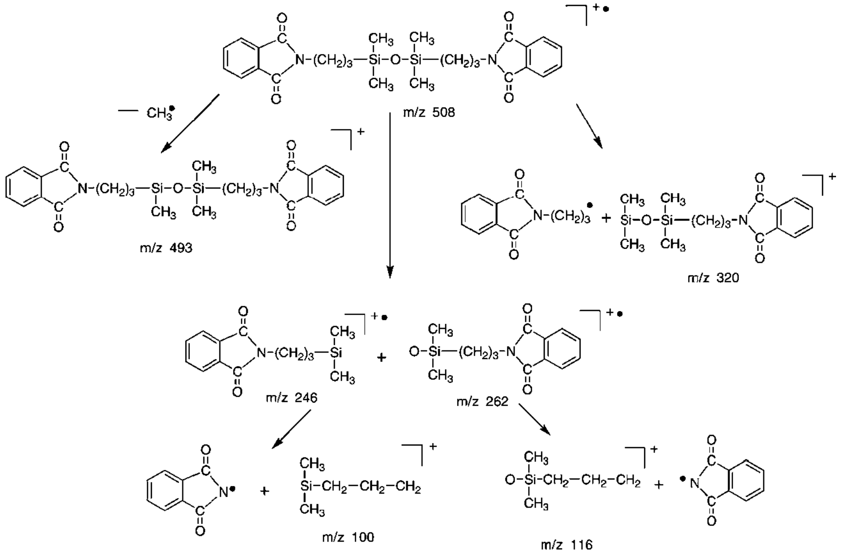

**FIGURE 3** EI mass fragmentation pattern for model compound B.

The spectrum of model compound A indicated that it was sufficiently stable at RT under the experimental conditions and that no chemical reactions occurred to cause any significant structural changes, as the spectra of the water-treated model compound A remained unchanged as that of untreated one. NMR spectra were recorded for compound A with 10% water after 8 h and one week of storage. It was observed that there was no significant change in their chemical shift positions as compared to untreated compound A with water. Therefore, it can be inferred that more drastic conditions other than presence of water are needed to bring about any noticeable change.

$^1$H-NMR spectrum for the compound SiDA is given in Figure 4, and it showed that the amine protons appeared at 2.6 ppm. However, in the spectra of model compound B (Figure 4 (a)), the peak corresponding to amine proton was absent at RT, confirming that the prepared compound B was free of unreacted amine and was pure. $^1$H-NMR spectra of compound B treated with 10 and 20% water at RT were recorded after 8 h and are given in Figure 4(b) and 4(c). A peak appearing at 2.8 ppm (Figure 4(b) and 4(c)) revealed the formation of $NH_2$, possibly due to the amide bond decomposition. This suggested that the model compound B was not stable at RT when compared to model compound A.

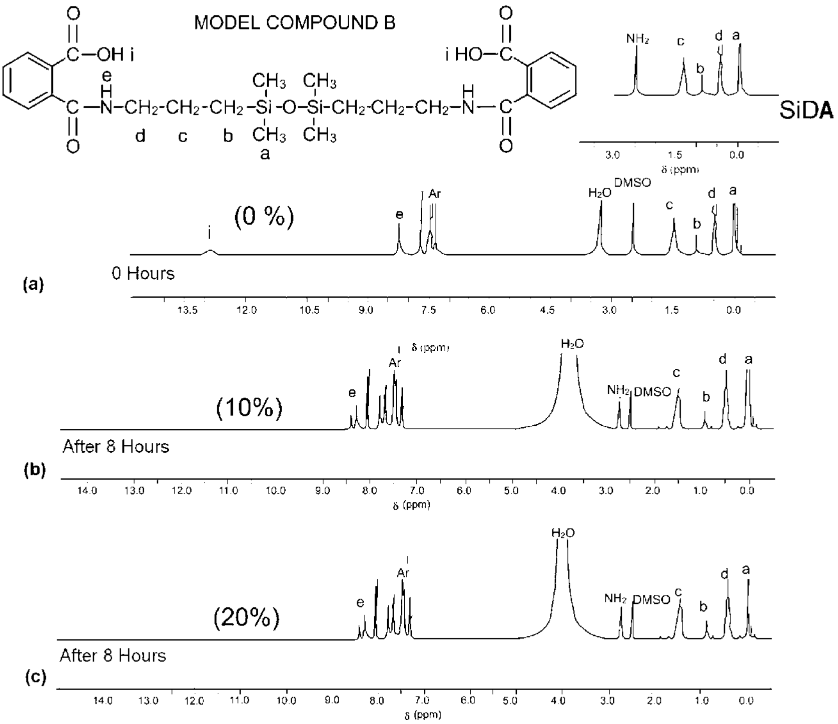

**FIGURE 4** $^1$H-NMR study of model compound B; effect of 0, 10, and 20% water content at RT.

## Bulk Viscosity of PAA, CoPAA, and CoPAS

Within the range of measurements, all shear rate dependence curves of CoPAS (with DEEM as well as DMEM) showed two viscous flow regions with quite different slopes. When the shear rate was less than 20 sec$^{-1}$, bulk viscosity decreased more with increasing shear rate. Then, bulk viscosity remained more or less stable from 20 to 38 sec$^{-1}$. Interestingly, however, for both the BPDA- and BTDA-based series of CoPAS with DMEM there was a sharper drop of viscosity in the shear rate range of 3 to 20 sec$^{-1}$. The decrease in viscosity with shear rate increase could be explained in terms of a stretching and disentangling of CoPAA chains in the viscous mass. At low shear rate, the polymer chain entanglements impede shear flow and viscosity is, therefore, high. As the shear rate increases, CoPAA chains orient and slip through each other in the direction of flow and disentangle from one another. In other words, the decrease of bulk viscosity with increasing shear rate was attributed to

**TABLE I** $E_a$ of Viscous Flow of CoPAA and CoPAS Determined at Constant Shear Rate as a Function of Temperature

| Copoly(amic acid) and photodefinable formulation composition | Activation energy of viscous flow (kJ/mol) | | |
|---|---|---|---|
| | CoPAA | CoPAS with DEEM | CoPAS with DMEM |
| BTDA-based CoPAA system | | | |
| [90% *o*-TDA + 10% SiDA] | 27.34 | 26.28 | 25.91 |
| [85% *o*-TDA + 15% SiDA] | 27.04 | 25.38 | 25.49 |
| [75% *o*-TDA + 25% SiDA] | 25.59 | 24.28 | 20.65 |
| BPDA-based CoPAA system | | | |
| [90% *o*-TDA + 10% SiDA] | 28.44 | 30.74 | 32.91 |
| [85% *o*-TDA + 15% SiDA] | 22.81 | 24.18 | 24.81 |
| [75% *o*-TDA + 25% SiDA] | 12.55 | 22.58 | 19.17 |

the gradually progressing disentangling of CoPAA chains due to shearing of solution.

Bulk viscosity of polymer solutions usually varies with shear temperature T[25,26]. At constant shear rate, bulk viscosity was measured as a function of temperature. Using an exponential Arrhenius-type relation given by:

$$\eta = \mathrm{A}\ \mathrm{e}^{\mathrm{Ea/RT}} \qquad (1)$$

The activation energy ($E_a$) of viscous flow was calculated by multiplying R with the slope of plots of ln $\eta$ versus [1/T]. Where $\eta$ is a viscosity, A is a pre-exponential factor, $E_a$ is an activation energy, R is a gas constant, and T is an absolute temperature.

Activation energies of viscous flow of BTDA-based CoPAA and CoPAS were in the range of 25–27 and 22–26 kJ/mol respectively, whereas BPDA-based CoPAA and CoPAS energies are in the range of 12–28 and 19–33 kJ/mol respectively (Table I). Activation energy of viscous flow decreased with increase in SiDA content for both CoPAA and CoPAS series. For a given composition, activation energy of viscous flow is comparable for DMEM- and DEEM-based CoPAS.

## Storage Stability Study of PAA, CoPAA, and CoPAS

Change in bulk viscosity of PAA, CoPAA, and CoPAS was monitored for one month during storage at RT. For bulk viscosity, the sample was tested once a week, whereas the inherent viscosity, molecular weight, and acid number were determined before and after one month of storage at RT. Bulk viscosity, inherent viscosity, molecular weight, and acid number decreased irrespective of the chemical composition and chemical structure of CoPAA and CoPAS (Tables II and III).

It has been reported that the PAA upon storage at RT undergoes equilibration reactions including propagation (forward), depolymerization, and hydrolysis as well as imidization[27–28]. Some PAA solutions were also found to undergo pseudogelation, which could be due to the physical association of polymer chains in the solution and the interaction between polymer and solvent[29]. If pseudogelation had taken place in the polymers under study, then bulk viscosity would have increased to well above 100,000 cP. However, it was not the case for these polymers. In fact, viscosity and molecular weights of these polymers drifted towards lower values (Tables II and III). The average rate of bulk viscosity drift of CoPAA based on BTDA was found to be 2.84 cP/h, and it was in the order of 1.62 order of magnitude higher than that of BPDA-based CoPAA. This behavior could be due to presence of a slightly higher amount of the polymer chain entanglements, thus maintaining viscous flow as indicated by the higher initial bulk viscosity of BPDA-based CoPAA, a semirigid polymer.

It has been reported that most reactive dianhydrides with high electron affinity (1.57 eV for BTDA and 1.38 eV for BPDA) values are most susceptible to undergoing side reactions upon storage[30–31]. This explanation holds true as evident for the higher viscosity drift of BTDA-than BPDA-based CoPAA systems.

As per the literature[4,32], the reactions, namely, (i) hydrolysis of PAA, (ii) imidization of PAA, and (iii) regeneration of dianhydride and diamine, might be taking place at RT. Out of these three reactions, the first two can be ruled out. The first reaction was ruled out because the acid number decreased in our study (Table III). Large-scale imidization was also less likely as its rate constant is two or three orders of magnitude less than that for the depolymerization reaction as well as that for amic acid hydrolysis. Hence, the second reaction is also ruled out. Therefore, the only feasible reaction is the dianhydride and diamine formation (i.e., reaction (iii)), which accounts for the decrease in acid number was well as decrease in bulk viscosity, molecular weights, and intrinsic viscosity. This argument is further supported by the appearance of amine peak in the NMR spectra of model compound B after 8 h (Figure 4). Because of the ability of SiDA moiety to regenerate amine more easily than that of *o*-TDA, the molecular weights, bulk viscosity, and inherent viscosity immediately after the synthesis, i.e., zero hour, were found to be lower as the SiDA content increased in the feed. Since there was no evidence for the formation of amine in model compound A even after one week, one can conclude that the weak linkage in the polymer chain was attributed to the SiDA moiety and not to the tolidine moiety.

**TABLE II** Solution Properties of PAA and PAS

| | Time interval of property monitoring (h) | | | | | | | | | | | | |
|---|---|---|---|---|---|---|---|---|---|---|---|---|---|
| | 0 | | | 672 | | | | | | | | | |
| | Molecular weights by GPC ($N \times 10^4$) | | | | | | 0 | 168 | 336 | 504 | 672 | 0 | 672 |
| Polymer composition and formulation | Mw | Mn | PD[a] | Mw | Mn | PD[a] | Bulk viscosity (cP) | | | | | Inh. viscosity (dl/g) | |
| [BTDA + *o*-TDA] | 7.18 | 4.28 | 1.68 | 3.65 | 2.57 | 1.42 | 12186 | 3615 | 2376 | 1905 | 1772 | 0.87 | 0.51 |
| [BTDA + *o*-TDA] PAA + DEEM | 7.37 | 4.45 | 1.66 | 4.60 | 3.02 | 1.52 | 19994 | 9564 | 6328 | 3881 | 3031 | 0.53 | 0.36 |
| [BTDA + *o*-TDA] PAA + DMEM | 7.41 | 4.60 | 1.61 | 4.81 | 3.15 | 1.53 | 18790 | 8714 | 5796 | 3707 | 2867 | 0.57 | 0.35 |
| [BPDA + *o*-TDA] | 6.44 | 3.86 | 1.67 | 4.99 | 3.17 | 1.58 | 21069 | 20378 | 19891 | 19200 | 18509 | 0.89 | 0.79 |
| [BPDA + *o*-TDA] PAA + DEEM | 6.15 | 3.76 | 1.64 | 4.40 | 2.84 | 1.54 | 36352 | 20403 | 15898 | 11750 | 10667 | 0.53 | 0.44 |
| [BPDA + *o*-TDA] PAA + DMEM | 6.24 | 3.78 | 1.65 | 4.59 | 2.95 | 1.56 | 32870 | 19866 | 15479 | 11913 | 9506 | 0.56 | 0.43 |
| [BTDA + SiDA] | 1.64 | 1.25 | 1.31 | 1.19 | 0.98 | 1.21 | 204 | 195 | 195 | 180 | 153 | 0.22 | 0.17 |
| [BPDA + SiDA] PAA + DEEM | 1.41 | 1.12 | 1.26 | 1.02 | 0.86 | 1.19 | 225 | 205 | 195 | 170 | 163 | 0.12 | 0.10 |
| [BPDA + SiDA] PAA + DMEM | 1.44 | 1.13 | 1.27 | 1.07 | 0.89 | 1.20 | 307 | 270 | 240 | 180 | 143 | 0.12 | 0.09 |
| [BPDA + SiDA] | 1.69 | 1.3 | 1.30 | 1.17 | 0.96 | 1.22 | 204 | 195 | 190 | 170 | 163 | 0.21 | 0.15 |
| [BPDA + SiDA] PAA + DEEM | 1.49 | 1.18 | 1.26 | 1.01 | 0.89 | 1.14 | 184 | 175 | 170 | 170 | 163 | 0.12 | 0.10 |
| [BPDA + SiDA] PAA + DMEM | 1.63 | 1.20 | 1.27 | 1.05 | 0.90 | 1.17 | 220 | 200 | 180 | 177 | 174 | 0.14 | 0.13 |

[a] Polydisperisty (*d*).

**TABLE III** Solution Properties of Co-PAA and Co-PAS

| | Analysis time (h) | | | | | | | | | | | |
|---|---|---|---|---|---|---|---|---|---|---|---|---|
| | 0 | | | 672 | | | | | | | | |
| | Molecular weight by GPC (N×10$^4$) | | | | | | 0 | 672 | 0 | 672 | 0 | 672 |
| Polymer composition and ionic salt formulation | Mw | Mn | PD[a] | Mw | Mn | PD[a] | Bulk viscosity (cp) | | Inh. viscosity (dl/g) | | Acid number[b] | |
| BTDA-based CoPAA | | | | | | | | | | | | |
| [90% *o*-TDA + 10% SiDA] | 6.47 | 4.35 | 1.49 | 3.91 | 2.83 | 1.38 | 3543 | 870 | 0.62 | 0.42 | 72.3 | 62.7 |
| [85% *o*-TDA + 15% SiDA] | 6.05 | 4.16 | 1.45 | 3.64 | 2.67 | 1.36 | 3197 | 645 | 0.60 | 0.39 | 72.7 | 62.2 |
| [75% *o*-TDA + 25% SiDA] | 5.53 | 3.83 | 1.44 | 3.38 | 2.54 | 1.33 | 1894 | 604 | 0.56 | 0.38 | 68.9 | 60.2 |
| BTDA-based CoPAA + DEEM | | | | | | | | | | | | |
| [90% *o*-TDA + 10% SiDA] | 5.32 | 3.76 | 1.41 | 3.67 | 2.71 | 1.35 | 1802 | 727 | 0.30 | 0.24 | 61.6 | 50.4 |
| [85% *o*-TDA + 15% SiDA] | 4.73 | 3.40 | 1.39 | 3.42 | 2.55 | 1.34 | 1321 | 634 | 0.28 | 0.23 | 57.5 | 50.7 |
| [75% *o*-TDA + 25% SiDA] | 4.03 | 2.98 | 1.35 | 3.08 | 2.32 | 1.33 | 1004 | 419 | 0.27 | 0.21 | 60.6 | 51.2 |
| BTDA-based CoPAA + DMEM | | | | | | | | | | | | |
| [90% *o*-TDA + 10% SiDA] | 4.82 | 3.46 | 1.39 | 3.54 | 2.62 | 1.35 | 7167 | 2949 | 0.30 | 0.23 | 60.4 | 48.1 |
| [85% *o*-TDA + 15% SiDA] | 4.67 | 3.35 | 1.39 | 2.79 | 2.10 | 1.32 | 1475 | 583 | 0.27 | 0.22 | 60.0 | 47.2 |
| [75% *o*-TDA + 25% SiDA] | 3.85 | 2.81 | 1.37 | 2.75 | 2.12 | 1.30 | 655 | 368 | 0.27 | 0.19 | 62.4 | 48.2 |

| | | | | | | | | | | | | |
|---|---|---|---|---|---|---|---|---|---|---|---|---|
| BPDA-based CoPAA | | | | | | | | | | | | |
| [90% *o*-TDA + 10% SiDA] | 5.57 | 3.90 | 1.43 | 3.64 | 2.65 | 1.37 | 2796 | 1024 | 0.55 | 0.43 | 73.7 | 63.2 |
| [85% *o*-TDA + 15% SiDA] | 4.64 | 3.29 | 1.41 | 3.61 | 2.66 | 1.36 | 1167 | 675 | 0.45 | 0.39 | 71.0 | 62.6 |
| [75% *o*-TDA + 25% SiDA] | 3.78 | 2.75 | 1.39 | 2.84 | 2.14 | 1.33 | 532 | 337 | 0.35 | 0.30 | 69.1 | 63.6 |
| BPDA-based CoPAA + DEEM | | | | | | | | | | | | |
| [90% *o*-TDA + 10% SiDA] | 5.16 | 3.70 | 1.40 | 3.38 | 2.50 | 1.35 | 3062 | 1126 | 0.31 | 0.25 | 59.7 | 55.0 |
| [85% *o*-TDA + 15% SiDA] | 4.80 | 3.46 | 1.39 | 3.19 | 2.37 | 1.35 | 1618 | 655 | 0.28 | 0.22 | 60.8 | 57.9 |
| [75% *o*-TDA + 25% SiDA] | 3.89 | 2.84 | 1.37 | 2.79 | 2.11 | 1.32 | 675 | 399 | 0.27 | 0.20 | 59.8 | 56.3 |
| BPDA-based CoPAA + DMEM | | | | | | | | | | | | |
| [90% *o*-TDA + 10% SiDA] | 5.31 | 3.76 | 1.41 | 3.73 | 2.73 | 1.37 | 1792 | 706 | 0.31 | 0.24 | 58.5 | 51.8 |
| [85% *o*-TDA + 15% SiDA] | 4.77 | 3.42 | 1.40 | 3.49 | 2.59 | 1.35 | 1290 | 593 | 0.28 | 0.22 | 64.8 | 51.6 |
| [75%*o*-TDA + 55% SiDA] | 4.06 | 2.97 | 1.37 | 3.14 | 2.35 | 1.34 | 952 | 471 | 0.25 | 0.21 | 59.7 | 54.4 |

[a] Polydispersity (*d*).
[b] mg of TMAH/g solution.

## WAXD Study of PAA, CoPAA, and CoPAS

WAXD curves showed that all the designed CoPAAs and CoPASs based on BTDA with DEEM and DMEM were amorphous.

## Solubility and Thermal Stability Study of PI and Co-PI

Both BPDA- and BTDA-based homo PI films were insoluble in the solvents tested, such as DCM, THF, NMP, acetone, DMAc, DMF, DMSO, and BLO. However, the extent of solubility of BTDA-based Co-PI films increased with increase in SiDA content in the feed, whereas BPDA-based Co-PI films became partially soluble with increase in SiDA content.

No $T_g$ was detected for [BTDA + *o*-TDA] PI film, and this was attributed to its structural rigidity. In the case of its copolymers, the rigidity decreased due to the presence of SiDA moiety, thus $T_g$ was observed for these copolymers and their films were flexible and self-supporting. Similarly, due to higher rigidity, no $T_g$ was observed up to 450°C for BPDA based polymer series, and their films were very brittle (Table IV).

Both PAA and CoPAA samples showed a two-step decomposition in air (Figure 5A(a)). During the first step, PAA or CoPAA underwent imidization to produce a PI or Co-PI, and the weight loss in the first step was attributed to the loss of water, whereas the second step was due to degradation of PI. In PAS or CoPAS during the first step, in addition to water of imidization, fragments of the photosensitive methacrylate compound were also liberated and PI was formed. On further heating, the formed PI degraded between 400 to 700°C. PI and CoPI films (Figure 5A(b)) showed a single step of decomposition. Five percent weight loss values of PI and Co-PI films are given in Table IV. The thermogram indicated that polymers were stable up to 350°C before any significant weight loss begun to occur. We have calculated the activation energy for the thermal degradation using Coats and Redfern[33] as well as Chang[34] methods.

In the Coats and Redfern[33] method, the plot of ln $[-\ln(1-\alpha)/T^2]$ versus $1/T$ gives a straight line with slope equivalent to $(-E_a/R)$ for a first-order reaction, where '$\alpha$' is the fraction decomposed at temperature '$T$,' '$\phi$' is heating rate, '$E_a$' is activation energy for the decomposition reaction, and '$R$' is universal gas constant.

Similarly in the Chang[34] method, the plot of ln $[(d\alpha/dt)/(1-\alpha)^n]$ against $[1/T]$ yields a straight line if the decomposition order n is selected correctly. The slope and intercept of this line provide the $(-E_a/R)$ and ln (A) values, respectively, where '$d\alpha/dt$' is the rate of fraction decomposed, '$\alpha$' is the fraction decomposed at temperature '$T$', '$E_a$' is activation energy for the

**TABLE IV** Solubility and Thermal Properties of PI and Co-PI Films

| | Solubility at RT | | | Thermal properties | | Activation energy *Ea* for thermal degradation (kJ/mol) | |
|---|---|---|---|---|---|---|---|
| Polymer composition | NMP | THF | Acetone | DSC Tg [°C] | TGA 5% wt. loss [°C] | Coats-Redfern method | Chang method |
| BTDA-based PI and CoPI system | | | | | | | |
| [BTDA + *o*-TDA] | — | — | — | N/D | 457.8 | 107.6 | 119.1 |
| [90% *o*-TDA + 10% SiDA] | — | — | — | 274 | 444.1 | 106.7 | 117.8 |
| [85% *o*-TDA + 15% SiDA] | ± | — | — | 252 | 438.8 | 101.6 | 112.4 |
| [75% *o*-TDA + 25% SiDA] | + | + | + | 249 | 421.4 | 98.4 | 106.4 |
| [BTDA + SiDA] | — | — | — | 179 | 402.5 | N/A | N/A |
| BPDA based PI and CoPI system | | | | | | | |
| [BPDA + *o*-TDA] | — | — | — | N/D | 492.9 | 139.6 | 133.7 |
| [90% *o*-TDA + 10% SiDA] | — | — | — | N/D | 453.6 | 93.2 | 92.2 |
| [85% *o*-TDA + 15% SiDA] | — | — | — | N/D | 431.6 | 73.2 | 76.4 |
| [75% *o*-TDA + 25% SiDA] | ± | ± | — | N/D | 416.1 | 65.6 | 75.0 |
| [BPDA + SiDA] | — | — | — | N/A | 492.9 | N/A | N/A |

Results Key: —: insoluble; ±: partially soluble; +: soluble; N/A: not available; N/D: not detectable.

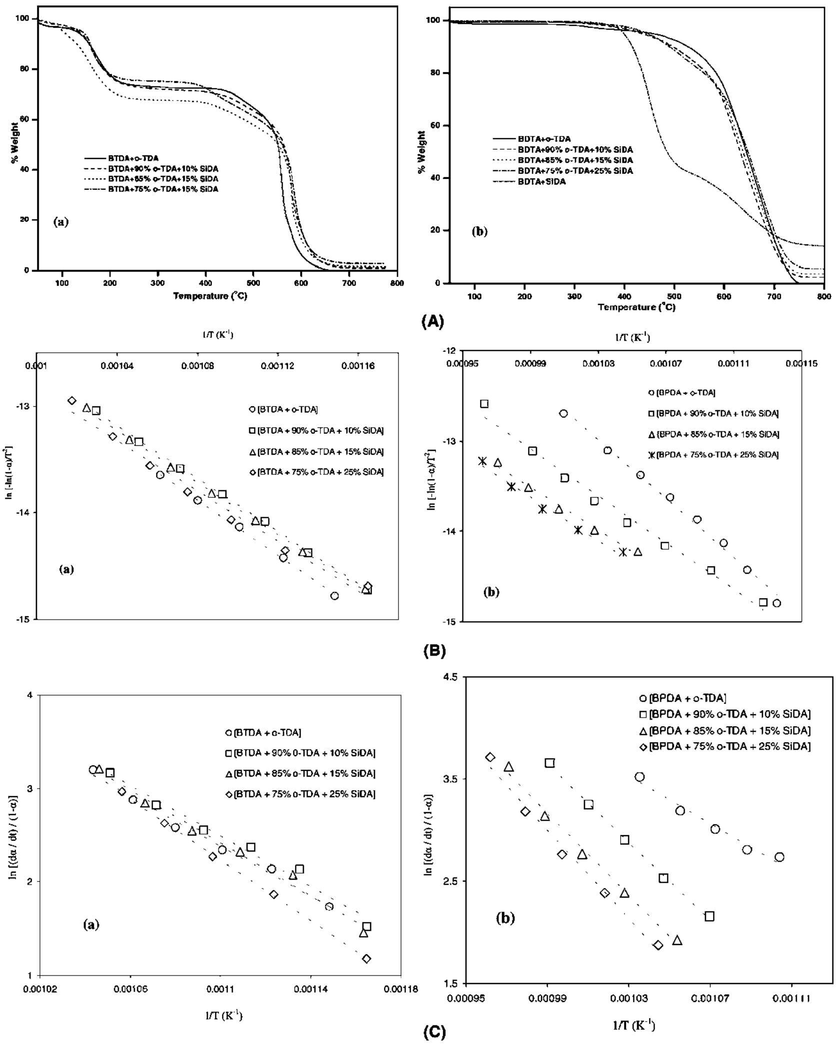

**FIGURE 5** (A) TGA thermogram of solid samples of (a) BTDA-based PAA and PAS with DEEM, (b) BTDA-based PI and CoPI films; (B) activation energy ($E_a$) calculated by the Coats and Redfern method for both (a) BTDA and (b) BPDA-based Co- PIs derived from solid CoPAS; (C) activation energy ($E_a$) calculated by the Chang method for both (a) BTDA and (b) BPDA-based Co-PIs derived from solid CoPAS.

decomposition reaction, 'R' is universal gas constant, and 'A' is Arrhenius frequency factor. A straight line was obtained when n is equal to one (Figure 5(B) and (C)). The results are tabulated in Table IV. $E_a$ determined by the Coats-Redfern method decreased by 8.5 and 53.0% as the SiDA content in the polymer increased to 25% in BTDA- and BPDA-based Co-PIs respectively. Similarly, for the Chang method, $E_a$ for thermal degradation decreased by 10.7 and 43.9% respectively with increase in SiDA content. It could be due to the presence of the thermally labile aliphatic propyl group in the SiDA moiety. This further confirmed that the poly(imide siloxane) polymers made from such aliphatic siloxane diamine are susceptible to thermal degradation faster than wholly aromatic PIs. The activation energy calculated by both methods was comparable.

## CONCLUSIONS

Bulk viscosity, molecular weights, inherent viscosity, and acid number of PAA, CoPAA, and CoPAS decreased upon storage at RT for a period of one month, irrespective of the chemical composition or the chemical structure of the Co-PAA, PAS, or CoPAS. This is explained on the basis of regeneration of diamine and dianhydride. The weak linkage was identified to be the amide bond between the dianhydride moiety and the aliphatic siloxane diamine (SiDA) moiety by $^1$H-NMR studies on model compounds. CoPAS was found to be less stable than Co-PAA. BPDA-based PAA showed less viscosity drift than the BTDA-based PAA. For BTDA-based polymer system, $T_g$ decreased as percent SiDA content increased. However, surprisingly, no $T_g$ was detectable for BPDA-based polymer system up to 450°C. Both DEEM- and DMEM-based CoPAS showed similar trend and showed distinct two-step weight losses. Imidization occurred from 50 to 350°C (removal of water and methacrylate group), followed by thermal degradation at higher temperatures. Activation energies for thermal degradation of both series of PIs films determined by the Coats-Redfern and Chang methods were comparable and decreased with increase in SiDA content.

## REFERENCES

[1] Mittal, K. L., ed. (1984). *Polyimides: Synthesis, Characterization, and Applications*, Vol. 1, pp. v. New York: Plenum Press.
[2] Xu, X. and M. R. Coleman. (1997). *J. Appl. Polym. Sci.*, **66**, 563.
[3] Maier, G. (2001). *Prog. Polym. Sci.*, **26**, 3.
[4] Omote, T. (1996). In *Polyimides: Fundamentals and Applications*, eds. M. K. Ghosh and K. L. Mittal, Ch. 5, pp. 121–149. New York: Marcel Dekker.
[5] Kolegov, V. I., V. P. Sklizkova, V. V. Kudryavtsev, B. G. Belen'kii, S. Y. Frenkel, and M. M. Koton. (1977). *Dokl. Akad. Nauk. USSR* (Engl. translation), **232**, 848.

[6] Laius, L. A. and M. I. Tsapovetsky. (1993). *Polyamic Acids and Polyimides: Synthesis, Transformation, and Structure*, eds. M. I. Bessonov and V. A. Zubkov, pp. 47–106. London: CRC Press.

[7] Bel'nikevich, N. G., V. M. Denisov, L. N. Korzhavin, and S. Y. Frankel. (1981). *Vysokomol. Soedin. Ser. A.,* **23**, 1268.

[8] Tong, Y., S. Veeramani, and R. H. Vora. (2001). In *Proceedings of the 6th World Congress on Chemical Engineering*, Melbourne, Section 3408, pp. 138.

[9] Olson, D. R. and E. A. O'Neil. (1991). U. S. Patent No. 5, 043, 418.

[10] Volksen, W. and P. M. Cotts. (1984). In *Polyimides: Synthesis, Characterization and Applications*, ed. K. L. Mittal, Vol. 1, pp 163–170. New York: Plenum Press.

[11] Krishnan, P. S. G., R. H. Vora, and T.-S. Chung. (2001). *Polymer*, **42**, 5165.

[12] Tong, Y., P. K. Pallathadka, and R. H. Vora. (2002). *Plast. Rubber Compos.*, **31**, 1.

[13] Krishnan, P. S. G., R. H. Vora, T.-S. Chung, S.-I. Uchimura, and N. Sasaki. (2004). *J. Polym Res. (Taiwan)*. (In press).

[14] Ree, M., T. L. Nunes, and K.-J. R. Chen. (1995). *J. Polym. Sci. Part B Polym. Phys.*, **33**, 453.

[15] Ree, M., T. L. Nunes, and J. S. Lin. (1994). *Polymer*, **35**, 1148.

[16] Han, H., J. Seo, M. Ree, S. M. Pyo, and C. C. Gryte. (1998). *Polymer*, **39**, 2963.

[17] Yoda, N. and H. Hiramoto. (1984). *J. Macromol. Sci. Chem. A.*, **21**, 1641.

[18] Asano, M., M. Eguchi, K. Kusano, and K. Niwa. (1993). *Polym. Adv. Technol.*, **4**, 261.

[19] Berger, A. and R. H. Vora. (1987). U.S. Patent No. 4, 681, 928.

[20] Hergenrother, P. M. and S. J. Havens. (1989). In *Polyimides: Materials, Chemistry, and Characterization*, eds. C. Feger, M. M. Khojasteh, and J. E. McGrath, pp. 45. New York: Elsevier.

[21] Summers, J. D., B. C. Auman, M. J. Grovola, and M. A. Guidry. (1999). In *Advances in Polyimides and Low Dielectric Polymers*, eds. H. S. Sachdev, M. M. Khojasteh, and C. Feger, pp. 131–152. Hopewell Junction, N.Y.: Society of Plastic Engineers.

[22] Vora, R. H., P. S. G. Krishnan, S. H. Goh, and T.-S. Chung. (2001). *Adv. Funct. Mater.*, **11**, 361.

[23] Vora, R. H. (1990). U. S. Patent No. 4, 933, 132.

[24] Krishnan, P. S. G., S. Veeramani, R. H. Vora, T.-S. Chung, S.-I. Uchimura, and H. Sugitani. (2002). *J. Chromatogr. A*, **977**, 207.

[25] Van Krevelen, D. W. (1990). *Properties of Polymers*, Ch. 16, pp. 499. New York: Elsevier.

[26] Takekoshi, T. (1996). In *Polyimides: Fundamental and Applications*, eds. M. K. Ghosh and K. L. Mittal, pp. 7–46. New York: Marcel Dekker.

[27] Kim, Y. J., T. E. Glass, G. D. Lyle, and J. E. McGrath. (1993). *Macromolecules*, **26**, 1344.

[28] Bessonov, M. I., M. M. Koton, V. V. Kudryavtsev, and L. A. Laius. (1987). *Polyimides—Thermally Stable Polymers*, pp. 1–318. New York: Plenum Press.

[29] Dine-Hart, R. A. and W. W. Wright. (1967). *J. Appl. Polym. Sci.*, **11**, 609.

[30] Frost, L. W. and I. Kesse. (1964). *J. Appl. Polym. Sci.*, **8**, 1039.

[31] Bender, M. L., Y. L. Chow, and F. Chluoek. (1958). *J. Am. Chem. Soc.*, **80**, 5380.

[32] Harris, F. W. (1990). In *Polyimides*, eds. D. Wilson, H. D. Stenzenberger, and P. M. Hergenrother, Ch. 1, pp. 1–298. New York: Chapman and Hall.

[33] Coats, A. W. and J. W. Redfern. (1965). *J. Polym. Sci. Part C Polym. Lett.*, **3**, 917.

[34] Chang, W. L. (1994). *J. Appl. Polym. Sci.*, **53**, 1759.